Genetic screening of ANXA11 revealed novel mutations linked to Amyotrophic Lateral Sclerosis

Elisa Teyssou, François Muratet, Maria-Del-Mar Amador, Mélanie Ferrien,
Géraldine Lautrette, Selma Machat, Séverine Boillée, Thierry Larmonier,
Safaa Saker, Éric Leguern, et al.

HAL Id: hal-03177242

https://hal.sorbonne-universite.fr/hal-03177242v1

Submitted on 23 Mar 2021

Genetic screening of *ANXA11* revealed novel mutations linked to Amyotrophic Lateral Sclerosis

Elisa Teyssou[1*], François Muratet[1*], Maria-Del-Mar Amador[1,2], Mélanie Ferrien[1], Géraldine Lautrette[3], Selma Machat[3], Séverine Boillée[1], Thierry Larmonier[4], Safaa Saker[4], Eric Leguern[1,5], Cécile Cazeneuve[5], Yannick Marie[1], Justine Guegan[1], Beata Gyorgy[1], Pascal Cintas[6], Vincent Meininger[7], Nadine Le Forestier[2,8], François Salachas[1,2], Philippe Couratier[3], William Camu[9], Danielle Seilhean[1,10*], Stéphanie Millecamps[1#*]

[1]Institut du Cerveau et de la Moelle épinière, ICM, Inserm U1127, CNRS UMR7225, Sorbonne Université, UPMC Univ Paris 6 UMRS1127, 75013 Paris, France

[2]Département de Neurologie, Assistance Publique Hôpitaux de Paris (APHP), Centre de référence SLA Ile de France, Hôpital de la Pitié-Salpêtrière, 75013 Paris, France

[3]Service de Neurologie, Centre de Référence SLA et autres maladies du neurone moteur, CHU de Limoges, 87000 Limoges, France

[4]Banque d'ADN et de cellules du Généthon, 91000 Evry, France

[5]Département de Génétique et Cytogénétique, Unité Fonctionnelle de neurogénétique moléculaire et cellulaire, APHP, Hôpital Pitié-Salpêtrière, 75013 Paris

[6]Département de Neurologie, Centre de référence SLA, CHU de Toulouse, 31000 Toulouse

[7]Hôpital des Peupliers, Ramsay Générale de Santé, 75013 Paris, France

[8]Département de recherche en éthique, EA 1610, Etudes des sciences et techniques, Université Paris Sud/Paris Saclay, 91400 Orsay, France

[9]Centre de référence SLA, Hôpital Gui de Chauliac, CHU et Université de Montpellier, 34000 Montpellier

[10]Département de Neuropathologie, APHP, Hôpital Pitié-Salpêtrière, 75013 Paris, France

*Equal contribution

#To whom correspondence should be addressed: Dr Stéphanie Millecamps, ICM, Hôpital Pitié-Salpêtrière, 47-83 Bd de l'Hôpital, CS21414, 75646 Paris Cedex, France, tel : 33157274341, e-mail: stephanie.millecamps@upmc.fr

Abstract

ANXA11 mutations have previously been discovered in Amyotrophic Lateral Sclerosis (ALS) motor neuron disease. To confirm the contribution of *ANXA11* mutations to ALS, a large exome dataset obtained from 330 French patients, including 150 familial ALS (FALS) index cases and 180 sporadic (SALS) cases, was analyzed, leading to the identification of 3 rare *ANXA11* variants in 5 patients. The novel p.L254V variant was associated to early onset SALS. The novel p.D40Y mutation and the p.G38R variant concerned patients with predominant pyramidal tract involvement and cognitive decline. Neuropathological findings in a p.G38R carrier associated the presence of ALS typical inclusions within the spinal cord, massive degeneration of the lateral tracts and type A Frontotemporal Lobar degeneration (FTLD). This mutant form of Annexin A11 accumulated in various brain regions and in spinal cord motor neurons, although its stability was decreased in patients' lymphoblasts. Since most ANXA11 inclusions were not colocalized with TDP-43 or p62 deposits, ANXA11 aggregation does not seem mandatory to trigger neurodegeneration with additional participants/partner proteins that could intervene.

Key words: ALS, Motor neuron disease, frontotemporal dementia, FTD, Annexin A11, ANXA11, neuropathology

Abbreviations: ALS: Amyotrophic Lateral Sclerosis, FALS: familial ALS; SALS: sporadic ALS, FTD: Frontotemporal Dementia.

Disclosure statement.

The authors declare no actual or potential conflicts of interest.

Highlights

- Novel ANXA11 mutations are responsible for ALS
- *ANXA11* mutations can be associated with early onset ALS and FTD
- Mutant p.G38R *ANXA11* is unstable in patient lymphoblasts
- Mutant p.G38R *ANXA11* led to cytoplasmic inclusions in post-mortem tissue

Introduction

High throughput sequencing applied to whole-genome or whole-exome (WGS/WES) analyses recently contributed to the discovery of novel genetic causes (including *VCP, PFN1, MATR3, CHCHD10, CCNF TUBA4A, TBK1, NEK1, C21orf2, KIF5A, GLT8D1* and *DNAJC7*) responsible for Amyotrophic Lateral Sclerosis (ALS) motor neuron disease. These novel genes have been identified using segregation studies in large ALS families or were found with excess of variants in ALS patients compared to controls using rare variant burden analysis (Johnson et al., 2010; Wu et al., 2012; Bannwarth et al., 2014; Johnson et al., 2014; Smith et al., 2014; Cirulli et al., 2015; Freischmidt et al., 2015; Brenner et al., 2016; Kenna et al., 2016; van Rheenen et al., 2016; Williams et al., 2016; Nicolas et al., 2018; Cooper-Knock et al., 2019; Farhan et al., 2019). An alternative recent exome analysis performed in 50 "multiplex" families (with DNA available for at least two members) from European origin, aimed to select genes with recurrent variants shared in several families but absent from control databases and selected *ANXA11* as the most promising novel ALS candidate gene (Smith et al., 2017). Further *ANXA11* analysis performed in 751 European familial (FALS) and 180 sporadic (SALS) cases identified a total of 6 different *ANXA11* mutations (p.G38R, p.D40G, p.G175R, p.G189E, p.R235Q, p.R346C) in 12 patients (including 9 from 6 families and 3 SALS cases), all with no Frontotemporal Dementia (FTD), accounting for 0.8% of FALS and 2% of SALS (Smith et al., 2017). In this study, the D40G mutation segregated in 2 distant relatives of 2 families and was also identified in another FALS index case and in 1 SALS patient (Smith et al., 2017).

Other *ANXA11* possible pathogenic mutations were identified in 3 independent Asian ALS cohorts compiling a total of 110 FALS, 1031 SALS and 12 ALS-FTD. These studies identified a recurrent P36R mutation in 4 patients (1 FALS and 3 SALS), the D40G mutation, already identified in Caucasian patients, in one SALS, 5 other missense mutations (p.V128M, p.S229R, p.A293V, p.I307M, p.Q362L) and one deletion (p.A58_Q187del) leading to the lack of the entire coding part of exon 6. Overall these mutations account for less than 1% of FALS and 0.1% of SALS in Asian populations (Tsai et al., 2018; Zhang et al., 2018; Liu et al., 2019). Two other missense variants p.R302C and p.G491R were also identified in these

3

studies. Although both of these variants were rare in ExAC browser (below the frequency of 0.005%), they were more frequently observed in gnomAD browser (frequency of 0.04% and 0.02%, respectively) suggesting a lower pathogenicity.

Patients with mutations in *ANXA11* presented a rather late onset of the disease (average 67 years, range 50-83 years), occurring at bulbar site for 5 out of 6 patients carrying the p.D40G mutation (Smith et al., 2017) and in patients with the p.P36R mutation (Zhang et al., 2018). One of these p.P36R patients also presented behavioral Frontotemporal Dementia (FTD) (Zhang et al., 2018).

ANXA11 gene encodes Annexin A11, a calcium-dependent phospholipid-binding protein with four conserved annexin domains in C terminus, able to bind to calcium ions, acidic phospholipids and phosphatidylethanolamine cell membrane components. Its long N terminus, rich in proline, glycine and tyrosine residues has the ability to bind to several partners including calcyclin (encoded by *S100A6*) and programmed cell death protein 6 (encoded by *PDCD6*). Through these interactions, Annexin A11 plays a role in cell division, Ca^{2+} signaling, vesicle trafficking and apoptosis (Wang et al., 2014). The dysregulation of Annexin A11 biological functions as well as the presence of the R230C variant in *ANXA11* (rs1049550) were incriminated in systemic autoimmune disease and sarcoidosis occurrence, and are associated with development, chemoresistance and recurrence of ovarian, breast, and colorectal cancers (Wang et al., 2014). ALS-linked *ANXA11* mutations were shown to modify interaction between Annexin A11 and calcyclin. This interaction was specifically inhibited by the p.D40G and p.G189E mutations and rather increased by the p.G38R mutation (Smith et al., 2017). Those modified binding properties were suggested to result in an accumulation of cytoplasmic Annexin A11 facilitating its aggregation (Smith et al., 2017). Annexin A11 was also recently found to mediate the docking of membraneless RNA granules on lysosomes for long distance trafficking and delivery of mRNA to distal locations within neurons, through its interaction with RNA on its N-terminal low-complexity region and with motile lysosomes on its C-terminus. ALS mutations (p.R235Q and p.R346C) were shown to impair this ability of Annexin A11 to associate with lysosomes (Liao et al., 2019).

Typical neuropathological features of ALS were observed in a p.D40G *ANXA11* mutation carrier including motor neuronal inclusions immunopositive for Transactive response DNA-binding 43 (TDP-43) and p62. Accumulations of Annexin A11 in skein-like, tubular-shaped and round inclusions were evidenced in the spinal cord, the motor cortex, the temporal cortex and occipital lobe of this patient. Some of these inclusions were ubiquitinated but did not colocalize with TDP-43. In contrast, no Annexin A11 accumulation was observed in healthy controls, ALS patients devoid of mutation in *ANXA11*, or patients with Alzheimer's or Parkinson's disease (Smith et al., 2017). Moreover calcyclin was overexpressed in astrocytes of the corticospinal tract in post-mortem tissues of ALS patients carrying or not a mutation in *ANXA11* (Smith et al., 2017).

To firmly link *ANXA11* mutations to ALS disease, we performed a genetic analysis of *ANXA11* in a large exome dataset obtained from French ALS patients including 200 FALS (150 index cases) and 180 SALS (100 SALS with early onset of the disease and 80 SALS patients with available post-mortem tissue) and studied ANXA11 levels in patient lymphoblasts and post-mortem tissue.

Methods

Patient cohort

All patients signed a consent form for the genetic research. Protocols were approved by the Medical Research Ethics Committee of "Assistance Publique Hôpitaux de Paris" (#A75). The diagnosis of ALS and FTD was based on published criteria as previously described (Teyssou et al., 2017). Autopsied patients were enrolled in the NeuroCEB brain donation program declared to the Ministry of Research and Universities, as requested by French Authorities (# AC-2013-1887). An explicit consent was signed by the patient himself, or by the next of kin, in the name of the patient, in accordance with the French Bioethical Laws. This document includes consent for genetic analyses.

Genetic analyses

This patient cohort (including 200 familial with 150 index cases and 180 sporadic cases with 100 patients with ALS onset before 35 years and 80 autopsied cases) was first screened for *C9orf72* and *ATXN2*

repeat expansions (Teyssou et al., 2017). Then Whole Exome Sequencing was performed using classical procedures. For FALS, exons were captured on the genomic DNA using the SureSelect Clinical Research Exome 50Mb kit (Agilent) followed by massive parallel sequencing on a Hiseq 2000 sequencer (Illumina) at Integragen (Evry, France). The Burrows-Wheeler algorithm was used to align the 100 bp length paired-end reads to the hg38 version of the human genome (Ensembl); variants were called using the Genome Analysis Toolkit (GATK) software. Data were imported into the SIRIUS (https://sirius.integragen.com) database for further analysis. For SALS, exons were captured from fragmented genomic DNA samples using the Nimblegen MedExome Enrichment kit (Roche) and paired-end 150-base massively parallel sequencing were carried out on an Illumina NextSeq 500 sequencer according to the manufacturer's protocols. Follow-up custom capture sequencing were performed with the KAPA hyperCap (Roche) to an average coverage of 100X within the captured regions with an average of 99% bases covered at least 5X. Bioinformatics analyses were carried out using the in-house pipeline. First a quality control of fastq files were done with FastQC. Low quality reads were trimmed or removed with trimmomatic. Reads were aligned to the Human Reference Genome (hg19) using the Burrows-Wheeler Alignment Tool (BWA). Picard software (http://picard.sourceforge.net/) was then used to remove duplicate reads. GenomeAnalysisTK-3.1-1 (GATK) was used to recalibrate base quality scores, realign around indels, call variants and recalibrate variant's score. Variants were annotated with ANNOVAR software (Wang et al., 2010). The depth of coverage was studied with GATK. Variants were visualized using graphical interfaces provided by the Bioinformaticians.

These exome databases were interrogated for 31 ALS related genes (including *ALS2, ANG, ANXA11, CCNF, CHCHD10, DAO, DCTN1, DNAJC7, FIG4, FUS, GLE1, GLT8D1, HNRNPA1, HNRNPA2B1, KIF5A, MATR3, NEK1, OPTN, PFN1, SETX, SIGMAR1, SOD1, SQSTM1, SS18L1, TARDBP, TBK1, TIA1, TUBA4A, UBQLN2, VAPB* and *VCP*) to select variants with a minor allele frequency (MAF) <0.005% in dbSNP, Hapmap, 1000genome, Exome Variant Server and gnomAD databases. *ANXA11* variants were validated using Sanger analysis with BigDye chemistry as recommended by the supplier (Applied

Biosystems). Segregation of the identified variant with the disease was checked for all family members with available DNA.

Lymphoblast cultures.

Lymphoblastoid cell lines from the ALS patients carrying the p.G38R, p.D40Y (2 patients) and p.L254V mutation were established by Epstein Barr virus transformation of peripheral blood mononuclear cells. Lymphoblasts from age-matched spouse/husbands were used as controls. Lymphoblasts were grown in RPMI 1640 supplemented with 10% fetal bovine serum, 50 U/ml penicillin and 50 mg/ml streptomycin (Life Technologies) renewed twice a week. Lymphoblasts (5.10^6 cells) were treated with 200 µg/ml cycloheximide (Sigma-Aldrich) or equivalent volume of dimethylsulfoxide (DMSO) in untreated group during 2, 4, 6 or 8 hours at 37°C for protein degradation assay and incubated at 42°C during 2 hours for heat-shock induction. For pellets, they were centrifuged 5 min at 3,000 rpm, rinsed in phosphate buffered saline (PBS) solution and frozen at -80°C.

Antibodies.

All primary antibodies were commercially available and included rabbit anti-Annexin A11 (10479-2-AP Proteintech), anti-S100A6 (Calcyclin, 10245-1-AP, Proteintech), anti-PDCD6 (12303-1-AP, Proteintech), anti-GAPDH (D16H11, Cell Signaling Technology), anti-TDP-43 (10782-2-AP, Proteintech), anti-Phosphorylated TDP-43 pS409/410-2 (TIP-PTD-P02, Cosmo Bio Co, LTD), anti-Cystatin C (HPA013143, Sigma Aldrich) and mouse anti-p62 (610833, BD Transduction Laboratories). Myelin Basic Protein/ Neurofilaments (MBP/NF) double labelling used anti-NF (2F11, Agilent) and anti-MBP (EP207, Bio Sb).

Western Blot analysis.

For immunoblots, cell pellets were homogenized in 50 mM Tris-HCl pH8, 150 mM NaCl, 1 mM $MgCl_2$, cOmplete™ Mini EDTA-free protease inhibitor cocktail and PhosStop phosphatase inhibitors and incubated at 37°C for 30 min with 0.5 U/µl Benzonase™ (all from Sigma-Aldrich). Sodium Dodecyl Sulfate (SDS) was added at a final concentration of 2% and cells were homogenized again. Protein extracts were centrifuged at 13,000 rpm for 10 min. Protein concentration of supernatants was estimated by the

bicinchoninic acid assay (Sigma-Aldrich). Proteins (15 µg) were separated on NuPAGE™ 4-12% Bis-Tris Gel (Life Technologies) and electrophoretically transferred to nitrocellulose membranes (PROTAN™, Whatman Gmbh). Membranes were incubated 3 hours with primary antibodies in PBS, 5% milk, 0.1% Tween 20, followed by one hour of incubation with peroxidase-conjugated goat anti-rabbit with minimal cross-reaction to human serum proteins (Jackson Immunoresearch Laboratories). Signals were detected using ECL™ Prime Western Blotting Detection Reagent (GE Healthcare Sa). Signal intensity was analyzed with MultiGauge 3.0 software.

Neuropathological examination

Three levels of spinal cord (cervical, thoracic, lumbar) were taken. Slides were stained with hematoxylin–eosin and Luxol fast blue. Immunostainings were performed after deparaffinization of 2 µm thick sections by an automatic slide stainer (Benchmark XT Ventana staining system). Slides were pre-treated at 95°C in CC1 (pH 8) proprietary retrieval buffer (Ventana Medical Systems). Antibodies were targeted with a biotin-free detection system (Ventana Medical Systems ultraView universal DAB Detection Kit coupled with the ultraView universal Alkaline Phosphatase Red Detection Kit for double staining).

Results

We identified 3 rare (with gnomAD minor allele frequency, MAF, below 0.005%) variants in *ANXA11* in 5 ALS patients including 3 familial (from 2 different families, Fig.S1) and 2 sporadic cases. Two of these variants: c.112G>A, p.Gly38Arg (p.G38R) and c.118G>T, p.Asp40Tyr (p.D40Y) were in the N-terminal low-complexity region (LCR) of Annexin A11 (Fig.1A-B) that is predicted to be a prion-like domain determined by the Prion Like Amino Acid Composition PLAAC software http://plaac.wi.mit.edu/ (King et al., 2012) and corresponding to the RNA binding domain of the protein (Liao et al., 2019). The c.760C>G, p.Leu254Val (p.L254V) is located in the C terminal Annexin region (Fig.1A-B) able to bind to lysosomes (Liao et al., 2019).

The p.D40Y and p.L254V *ANXA11* mutations are 2 novel variants absent from control and ALS patients databases (Table 1). The p.G38R variant was reported with a MAF of 0.0077 % in controls (non Finnish

European population of gnomAD) and of 0.06-0.09% in ALS patient databases (in ALSdb and project MinE data browser, respectively).

Additionally a c.629G>A, p. Arg210Gln (p.R210Q) variant was identified in 2 other unrelated FALS (Fig.1, Table 1, Fig.S1). The reported MAF for this *ANXA11* variant was 0.1% in non Finnish European population in gnomAD browser and was similar in ALS patients and controls in Project MinE data browser (Table 1). Moreover both patients with this p.R210Q ANXA11 variant also carried a variant in another ALS-related gene including *TBK1*, c.427C>T, p.Arg143Cys, p.R143C (FALS3II1) or *GLE1*, c.1858A>G, p.Thr620Ala, p.T620A (FALS4II1, Table 2). The *TBK1* p.R143C variant was already identified in the project MinE data browser and concerned 0.012% of ALS cases but no controls. The *GLE1* p.T620A is a novel variant absent from public databases. From these genetic results we concluded that the *ANXA11* R210Q variant was less pathogenic than the 3 other *ANXA11* variants we identified and is a variant of unknown significance.

All these *ANXA11* variants were predicted to be deleterious using 5 *in silico* software packages (Table 1) and affect a residue that is conserved through mammals (Fig.1C).

Each of the p.G38R, p.D40Y and p.R210Q variants were identified in 2 different patients (who were siblings for the p.D40Y mutation) and all had disease onset after the age of 56 (Table 2). The p.L254V variant was associated to early onset ALS phenotype, which occurred at 33 years of age in an apparently sporadic case (with 8 siblings and whose father accidently died at the age of 40). Disease evolution ranged between 9 and 67 months for *ANXA11* patients. Patients with p.G38R mutation presented ALS with predominant pyramidal tract involvement of all limbs (important spasticity for 2 of them) as well as frontal cognitive dysfunction meeting the criteria of FTD for 2 of them (Table 2). A similar phenotype was observed for both patients with the p.D40Y mutation who both presented behavioral dementia (Table 2).

To study the functional impact of the *ANXA11* mutations we identified, lymphoblastoid cell lines were established from lymphocytes for the ALS patients carrying the p.D40Y and the p.L254V mutations and

9

were compared to lymphoblastoid cell lines carrying the known p.G38R mutation or to healthy controls. Western blot analyses showed that the p.G38R mutation impacted the Annexin A11 protein expression levels, which were decreased, compared to controls (Fig.2A-B). To determine whether the loss of p.G38R mutant form of Annexin A11 could result from protein instability, we treated patient lymphoblasts with cycloheximide and measured the time course of Annexin A11 levels 2 to 8 hours after starting this treatment. This protein degradation assay showed an accelerated degradation kinetic in lymphoblasts carrying the p.G38R mutant form compared to others. No such loss of stability of Annexin A11 was measured for the p.D40Y and the p.L254V mutation in patient lymphoblasts. To determine whether levels of Annexin A11 were modified after cellular stress, we exposed patient lymphoblasts to heat shock and measured levels of Annexin A11. These protein levels did not change after heat shock for controls or patients carrying *ANXA11* mutations (Fig.S2). In addition, we measured protein levels of Annexin A11 partners in control and patient lymphoblasts. Equal levels of PDCD6 were detected in mutant and control lymphoblasts (Fig.S3). In contrast, S100A6 levels were increased in p.G38R and p.L254V compared to controls and p.D40Y lymphoblasts (Fig.2C).

Post-mortem tissues were available for one p.G38R *ANXA11* variant carrier. This case was characterized by severe damage of the lateral tracts (Fig.3S-T) and of the primary motor cortex with loss of Betz cells. In the frontal, temporal and parietal isocortices, as well as in the superficial motor cortex, neuronal loss was moderate. The intraneuronal and glial p62 and TDP-43 positive inclusions were numerous, intracytoplasmic, either rounded and paranuclear, or surrounding the nucleus like a ring (Fig.3A-B, 3F-G). They were distributed in layer 2 of the cortex and were associated with positive short neuritis, evoking Mackenzie type A distribution (Mackenzie et al., 2011). TDP-43 and p62 inclusions were also observed in the dentate gyrus of the hippocampus (Fig.3C, 3H) and the head of caudate nucleus (Fig.3D, 3I). In the dentate nucleus of the cerebellum, some TDP-43 cytoplasmic inclusions were observed (Fig.3E). No p62 accumulation was noted in this region, except rare glial dot-like staining (Fig.3J arrowheads). No TDP-43 or p62 staining was evidenced in the granular or Purkinje cells of the cerebellum.

Annexin A11 positive inclusions were found in all brain areas examined including the superficial motor cortex, midfrontal and superior temporal isocortices, hippocampus, caudate nucleus, mesencephalon and dentate nucleus of the cerebellum (Fig.3K-O). The distribution of ANXA11-positive deposits followed that of TDP-43 and p62 in all brain areas examined, except for the cerebellum where the lesions were only stained by TDP-43 and/or ANXA11.

In the spinal cord, anti-Cystatin C immunohistochemistry showed typical Bunina bodies in motor neurons (Fig.4A-B). Skein-like inclusions, immunopositive for p62 and TDP-43, were observed (Fig.4E-H). Deposits of p62 and TDP-43 were also visible in some glial cells. Some ANXA11 tubular-shaped deposits mimicked those skein-like inclusions (Fig.4C-D). Double staining for ANXA11/TDP-43 or ANXA11/p62 showed intermingled positivity for ANXA11 with either TDP-43 or p62 with no clear superposition (Fig.3P-R, 3U-W arrows and arrow heads, 4O-P). Accumulations of ANXA11 were observed in neurons having retained their nuclear TDP-43 immunoreactivity (Fig.4I) or on the contrary having lost it (Fig.3P). However, a superposition of ANXA11 and TDP-43 (Fig.4M-N), or ANXA11 and p62 (Fig.3W star), could be observed in intracytoplasmic conglomerates. An increased staining for S100A6 was previously reported in a D40G *ANXA11* mutation carrier and was also observed in ALS patients with no mutation in *ANXA11* (Smith et al., 2017). Such an increased S100A6 staining was also observed for the p.G38R *ANXA11* carrier in the lateral tracts corresponding to an astroglial cytoplasmic positivity (Fig.3X-Y arrows), as well as in the other ALS patients we analyzed (including 2 sporadic cases and 2 patients carrying the *C9orf72* repeat expansion).

No abnormal periodic acid schiff (PAS) positive material, that would have suggested a significant lysosomal dysfunction (Steven U Walkley, 2008), was detected in any cerebral region of the p.G38R patient tissue.

Discussion

We analyzed *ANXA11* gene mutation in a large population of ALS patients. The p.L254V and p.D40Y mutations were probably pathogenic as they were absent from control databases. Moreover the p.D40Y

mutation segregated in the concerned family in 2 siblings and affects the same amino acid residue than the D40G mutation already described. We also identified the p.G38R *ANXA11* mutation in two ALS patients (1 FALS and 1 SALS). Although this variant had been detected in 8 out of 51,915 NFE individuals in gnomAD database, it had already been described in two unrelated FALS patients (Smith et al., 2017) and was present in 4 out of 3317 ALS patients from the ALSdb sequencing data.

ALS phenotype of these *ANXA11* patients differed slightly from the one described for the D40G *ANXA11* variant (Smith et al., 2017), both in the mode of onset and in the predominance of clinical deficits. The disease occurred early for the p.L254V mutation and, for the p.G38R and p.D40Y, it was associated with FTD and major pyramidal impairment (leading to severe spasticity in 3 cases). Cognitive impairment was previously reported for one Asian patient having the P36R *ANXA11* mutation (Zhang et al., 2018), a variant located close to the p.G38R mutation carried by our patient.

The neuropathological analysis we performed for the p.G38R case correlated with the clinical presentation and ascertained (i) the presence of ALS typical inclusions within the spinal cord, usually observed for example in sporadic ALS cases or in ALS cases carrying the *C9orf72* repeat expansion (Saberi et al., 2015), (ii) massive degeneration of the lateral tracts and (iii) accumulation of numerous TDP-43 lesions in the cortex evoking a Frontotemporal Lobar Degeneration (FTLD)-TDP type A distribution (Mackenzie et al., 2011). Such TDP-43 lesion distribution is unusual in ALS patients as it is rather associated with pure FTD phenotype, either behavioral, related to non-fluent aphasia or linked to *GRN* or *C9orf72* mutation (Mackenzie et al., 2014).

Our neuropathological analysis also showed that mutant Annexin A11 protein accumulated within different neuronal types. Topography of the lesions followed those of TDP-43 and p62 and are quite similar to that described in a patient with the p.D40G *ANXA11* mutation (Smith et al., 2017). Compiled with this previous study, our results suggest typical neuropathological features shared by *ANXA11* mutations.

In addition, we observed some ANXA11 inclusions in the dentate nucleus of the cerebellum which paralleled TDP-43 deposits. Double staining of Annexin A11 with TDP-43 or p62 showed various stages

of protein aggregation in neurons. TDP-43 and p62 accumulation occurred even in the absence of any Annexin A11 deposit. This suggested that Annexin A11 aggregation is not mandatory to trigger the neurodegenerative process and that other participants/partner proteins should intervene.

The protein accumulations we observed in p.G38R patient tissue were not correlated to the protein levels measured in patient lymphoblasts. Indeed, in these cells the level of Annexin A11 was lower with the p.G38R mutation. This was due, at least in part, to the instability of this mutant protein in this cell type, as shown by the protein degradation assay we performed. Such reduced protein stability was previously reported for the p.G38R and p.D40G *ANXA11* mutations after surexpression of these mutant forms in HEK293 cells (Liao et al., 2018).

As no blood and/or cerebrospinal fluid (CSF) were taken from patients carrying ANXA11 variants we described in the present study, we could not measure Annexin A11 levels in these fluids. Whether these levels are modified in ANXA11 patients remained to be determined.

Decreased stability of a mutant protein associated with paradoxal protein accumulations in patient tissue is a well-documented outcome for mutations in *SOD1*, the first discovered genetic causes of ALS. Indeed analysis of protein stability of 22 different SOD1 mutations evidenced increased protein instability for most (but not all) of them using patient erythrocytes (Sato et al., 2005). Nevertheless some of these unstable mutated forms of SOD1 can accumulate in neurons of transgenic mice (Bruijn et al., 1997; Joyce et al., 2015) and in motor neurons of ALS patients (Shibata et al., 1996). It has been proposed that the formation of SOD1 aggregates could result from post-translational modifications of the SOD1 dimers or their dissociation into monomers. Indeed the most unstable form of the mutant SOD1 relative to the wild-type (WT) SOD1 protein is the disulfide-reduced immature form, which is also the most prone to oligomerization through disulfide cross-linking process upon mild oxidative stress (Furukawa and O'Halloran, 2005). This disulfide cross-linking process for SOD1 is tissue specific as it occurs in spinal cord of mouse models but was not observed in unaffected tissue (Furukawa et al., 2006). Disulfide mutant cross-linked SOD1 species were shown to have the ability to incorporate WT SOD1 protein (Furukawa et al., 2006). This

heterodimer formation protects mutant SOD1 from degradation (Weichert et al., 2014) and promotes the formation of SOD1 inclusions (Brasil et al., 2019). Interestingly, the p.R235Q *ANXA11* mutation, that is prone to aggregate, was shown to be able to sequester WT Annexin A11 through a dominant-negative toxic effect (Smith et al., 2017). Whether any post-translational modification could influence mutant ANXA11 folding and aggregation remains to be investigated.

Overall, our study confirmed the contribution of *ANXA11* mutations to ALS and ALS-FTD and proved the pathogenicity of the *ANXA11* p.G38R mutation, despite its frequency reported in control populations, based on neuropathological observations.

References

Bannwarth S, Ait-El-Mkadem S, Chaussenot A, Genin EC, Lacas-Gervais S, Fragaki K, Berg-Alonso L, Kageyama Y, Serre V, Moore DG, Verschueren A, Rouzier C, Le Ber I, Auge G, Cochaud C, Lespinasse F, N'Guyen K, de Septenville A, Brice A, Yu-Wai-Man P, Sesaki H, Pouget J, Paquis-Flucklinger V (2014) A mitochondrial origin for frontotemporal dementia and amyotrophic lateral sclerosis through CHCHD10 involvement. Brain 137:2329-2345.

Brasil AA, de Carvalho MDC, Gerhardt E, Queiroz DD, Pereira MD, Outeiro TF, Eleutherio ECA (2019) Characterization of the activity, aggregation, and toxicity of heterodimers of WT and ALS-associated mutant Sod1. Proc Natl Acad Sci U S A 116:25991-26000.

Brenner D, Muller K, Wieland T, Weydt P, Bohm S, Lule D, Hubers A, Neuwirth C, Weber M, Borck G, Wahlqvist M, Danzer KM, Volk AE, Meitinger T, Strom TM, Otto M, Kassubek J, Ludolph AC, Andersen PM, Weishaupt JH (2016) NEK1 mutations in familial amyotrophic lateral sclerosis. Brain 139:e28.

Bruijn LI, Becher MW, Lee MK, Anderson KL, Jenkins NA, Copeland NG, Sisodia SS, Rothstein JD, Borchelt DR, Price DL, Cleveland DW (1997) ALS-linked SOD1 mutant G85R mediates damage to astrocytes and promotes rapidly progressive disease with SOD1-containing inclusions. Neuron 18:327-338.

Cirulli ET, Lasseigne BN, Petrovski S, Sapp PC, Dion PA, Leblond CS, Couthouis J, Lu YF, Wang Q, Krueger BJ, Ren Z, Keebler J, Han Y, Levy SE, Boone BE, Wimbish JR, Waite LL, Jones AL, Carulli JP, Day-Williams AG, Staropoli JF, Xin WW, Chesi A, Raphael AR, McKenna-Yasek D,

Cady J, Vianney de Jong JM, Kenna KP, Smith BN, Topp S, Miller J, Gkazi A, Al-Chalabi A, van den Berg LH, Veldink J, Silani V, Ticozzi N, Shaw CE, Baloh RH, Appel S, Simpson E, Lagier-Tourenne C, Pulst SM, Gibson S, Trojanowski JQ, Elman L, McCluskey L, Grossman M, Shneider NA, Chung WK, Ravits JM, Glass JD, Sims KB, Van Deerlin VM, Maniatis T, Hayes SD, Ordureau A, Swarup S, Landers J, Baas F, Allen AS, Bedlack RS, Harper JW, Gitler AD, Rouleau GA, Brown R, Harms MB, Cooper GM, Harris T, Myers RM, Goldstein DB (2015) Exome sequencing in amyotrophic lateral sclerosis identifies risk genes and pathways. Science.

Cooper-Knock J, Moll T, Ramesh T, Castelli L, Beer A, Robins H, Fox I, Niedermoser I, Van Damme P, Moisse M, Robberecht W, Hardiman O, Panades MP, Assialioui A, Mora JS, Basak AN, Morrison KE, Shaw CE, Al-Chalabi A, Landers JE, Wyles M, Heath PR, Higginbottom A, Walsh T, Kazoka M, McDermott CJ, Hautbergue GM, Kirby J, Shaw PJ (2019) Mutations in the Glycosyltransferase Domain of GLT8D1 Are Associated with Familial Amyotrophic Lateral Sclerosis. Cell Rep 26:2298-2306 e2295.

Farhan SMK, Howrigan DP, Abbott LE, Klim JR, Topp SD, Byrnes AE, Churchhouse C, Phatnani H, Smith BN, Rampersaud E, Wu G, Wuu J, Shatunov A, Iacoangeli A, Al Khleifat A, Mordes DA, Ghosh S, Eggan K, Rademakers R, McCauley JL, Schule R, Zuchner S, Benatar M, Taylor JP, Nalls M, Gotkine M, Shaw PJ, Morrison KE, Al-Chalabi A, Traynor B, Shaw CE, Goldstein DB, Harms MB, Daly MJ, Neale BM (2019) Exome sequencing in amyotrophic lateral sclerosis implicates a novel gene, DNAJC7, encoding a heat-shock protein. Nat Neurosci.

Freischmidt A, Wieland T, Richter B, Ruf W, Schaeffer V, Muller K, Marroquin N, Nordin F, Hubers A, Weydt P, Pinto S, Press R, Millecamps S, Molko N, Bernard E, Desnuelle C, Soriani MH, Dorst J, Graf E, Nordstrom U, Feiler MS, Putz S, Boeckers TM, Meyer T, Winkler AS, Winkelman J, de Carvalho M, Thal DR, Otto M, Brannstrom T, Volk AE, Kursula P, Danzer KM, Lichtner P, Dikic I, Meitinger T, Ludolph AC, Strom TM, Andersen PM, Weishaupt JH (2015) Haploinsufficiency of TBK1 causes familial ALS and fronto-temporal dementia. Nat Neurosci 18:631-636.

Furukawa Y, O'Halloran TV (2005) Amyotrophic lateral sclerosis mutations have the greatest destabilizing effect on the apo- and reduced form of SOD1, leading to unfolding and oxidative aggregation. J Biol Chem 280:17266-17274.

Furukawa Y, Fu R, Deng HX, Siddique T, O'Halloran TV (2006) Disulfide cross-linked protein represents a significant fraction of ALS-associated Cu, Zn-superoxide dismutase aggregates in spinal cords of model mice. Proc Natl Acad Sci U S A 103:7148-7153.

Johnson JO, Mandrioli J, Benatar M, Abramzon Y, Van Deerlin VM, Trojanowski JQ, Gibbs JR, Brunetti M, Gronka S, Wuu J, Ding J, McCluskey L, Martinez-Lage M, Falcone D, Hernandez DG, Arepalli S, Chong S, Schymick JC, Rothstein J, Landi F, Wang YD, Calvo A, Mora G, Sabatelli M, Monsurro MR, Battistini S, Salvi F, Spataro R, Sola P, Borghero G, Galassi G, Scholz SW, Taylor JP, Restagno G, Chio A, Traynor BJ (2010) Exome sequencing reveals VCP mutations as a cause of familial ALS. Neuron 68:857-864.

Johnson JO, Pioro EP, Boehringer A, Chia R, Feit H, Renton AE, Pliner HA, Abramzon Y, Marangi G, Winborn BJ, Gibbs JR, Nalls MA, Morgan S, Shoai M, Hardy J, Pittman A, Orrell RW, Malaspina A, Sidle KC, Fratta P, Harms MB, Baloh RH, Pestronk A, Weihl CC, Rogaeva E, Zinman L, Drory VE, Borghero G, Mora G, Calvo A, Rothstein JD, Drepper C, Sendtner M, Singleton AB, Taylor JP, Cookson MR, Restagno G, Sabatelli M, Bowser R, Chio A, Traynor BJ (2014) Mutations in the Matrin 3 gene cause familial amyotrophic lateral sclerosis. Nat Neurosci 17:664-666.

Joyce PI, McGoldrick P, Saccon RA, Weber W, Fratta P, West SJ, Zhu N, Carter S, Phatak V, Stewart M, Simon M, Kumar S, Heise I, Bros-Facer V, Dick J, Corrochano S, Stanford MJ, Luong TV, Nolan PM, Meyer T, Brandner S, Bennett DL, Ozdinler PH, Greensmith L, Fisher EM, Acevedo-Arozena A (2015) A novel SOD1-ALS mutation separates central and peripheral effects of mutant SOD1 toxicity. Hum Mol Genet 24:1883-1897.

Kenna KP, van Doormaal PT, Dekker AM, Ticozzi N, Kenna BJ, Diekstra FP, van Rheenen W, van Eijk KR, Jones AR, Keagle P, Shatunov A, Sproviero W, Smith BN, van Es MA, Topp SD, Kenna A, Miller JW, Fallini C, Tiloca C, McLaughlin RL, Vance C, Troakes C, Colombrita C, Mora G, Calvo A, Verde F, Al-Sarraj S, King A, Calini D, de Belleroche J, Baas F, van der Kooi AJ, de Visser M, Ten Asbroek AL, Sapp PC, McKenna-Yasek D, Polak M, Asress S, Munoz-Blanco JL, Strom TM, Meitinger T, Morrison KE, Lauria G, Williams KL, Leigh PN, Nicholson GA, Blair IP, Leblond CS, Dion PA, Rouleau GA, Pall H, Shaw PJ, Turner MR, Talbot K, Taroni F, Boylan KB, Van Blitterswijk M, Rademakers R, Esteban-Perez J, Garcia-Redondo A, Van Damme P, Robberecht W, Chio A, Gellera C, Drepper C, Sendtner M, Ratti A, Glass JD, Mora JS, Basak NA, Hardiman O, Ludolph AC, Andersen PM, Weishaupt JH, Brown RH, Jr., Al-Chalabi A, Silani V, Shaw CE, van den Berg LH, Veldink JH, Landers JE (2016) NEK1 variants confer susceptibility to amyotrophic lateral sclerosis. Nat Genet 48:1037-1042.

King OD, Gitler AD, Shorter J (2012) The tip of the iceberg: RNA-binding proteins with prion-like domains in neurodegenerative disease. Brain Res 1462:61-80.

Liao D, Liao Q, Huang C, Bi F (2018) [Mutations of G38R and D40G cause amyotrophic lateral sclerosis by reducing Annexin A11 protein stability]. Zhong Nan Da Xue Xue Bao Yi Xue Ban 43:577-582.

Liao YC, Fernandopulle MS, Wang G, Choi H, Hao L, Drerup CM, Patel R, Qamar S, Nixon-Abell J, Shen Y, Meadows W, Vendruscolo M, Knowles TPJ, Nelson M, Czekalska MA, Musteikyte G, Gachechiladze MA, Stephens CA, Pasolli HA, Forrest LR, St George-Hyslop P, Lippincott-Schwartz J, Ward ME (2019) RNA Granules Hitchhike on Lysosomes for Long-Distance Transport, Using Annexin A11 as a Molecular Tether. Cell 179:147-164 e120.

Liu X, Wu C, He J, Zhang N, Fan D (2019) Two rare variants of the ANXA11 gene identified in Chinese patients with amyotrophic lateral sclerosis. Neurobiol Aging 74:235 e9-235 e212.

Mackenzie IR, Frick P, Neumann M (2014) The neuropathology associated with repeat expansions in the C9ORF72 gene. Acta Neuropathol 127:347-357.

Mackenzie IR, Neumann M, Baborie A, Sampathu DM, Du Plessis D, Jaros E, Perry RH, Trojanowski JQ, Mann DM, Lee VM (2011) A harmonized classification system for FTLD-TDP pathology. Acta Neuropathol 122:111-113.

Nicolas A, Kenna KP, Renton AE, Ticozzi N, Faghri F, Chia R, Dominov JA, Kenna BJ, Nalls MA, Keagle P, Rivera AM, van Rheenen W, Murphy NA, van Vugt J, Geiger JT, Van der Spek RA, Pliner HA, Shankaracharya, Smith BN, Marangi G, Topp SD, Abramzon Y, Gkazi AS, Eicher JD, Kenna A, Mora G, Calvo A, Mazzini L, Riva N, Mandrioli J, Caponnetto C, Battistini S, Volanti P, La Bella V, Conforti FL, Borghero G, Messina S, Simone IL, Trojsi F, Salvi F, Logullo FO, D'Alfonso S, Corrado L, Capasso M, Ferrucci L, Moreno CAM, Kamalakaran S, Goldstein DB, Gitler AD, Harris T, Myers RM, Phatnani H, Musunuri RL, Evani US, Abhyankar A, Zody MC, Kaye J, Finkbeiner S, Wyman SK, LeNail A, Lima L, Fraenkel E, Svendsen CN, Thompson LM, Van Eyk JE, Berry JD, Miller TM, Kolb SJ, Cudkowicz M, Baxi E, Benatar M, Taylor JP, Rampersaud E, Wu G, Wuu J, Lauria G, Verde F, Fogh I, Tiloca C, Comi GP, Soraru G, Cereda C, Corcia P, Laaksovirta H, Myllykangas L, Jansson L, Valori M, Ealing J, Hamdalla H, Rollinson S, Pickering-Brown S, Orrell RW, Sidle KC, Malaspina A, Hardy J, Singleton AB, Johnson JO, Arepalli S, Sapp PC, McKenna-Yasek D, et al. (2018) Genome-wide Analyses Identify KIF5A as a Novel ALS Gene. Neuron 97:1268-1283 e1266.

Rentzsch, P., Witten, D., Cooper, G.M., Shendure, J., Kircher, M., 2019. CADD: predicting the deleteriousness of variants throughout the human genome. Nucleic Acids Res. 47, D886eD894.

Saberi S, Stauffer JE, Schulte DJ, Ravits J (2015) Neuropathology of Amyotrophic Lateral Sclerosis and Its Variants. Neurol Clin 33:855-876.

Sato T, Nakanishi T, Yamamoto Y, Andersen PM, Ogawa Y, Fukada K, Zhou Z, Aoike F, Sugai F, Nagano S, Hirata S, Ogawa M, Nakano R, Ohi T, Kato T, Nakagawa M, Hamasaki T, Shimizu

A, Sakoda S (2005) Rapid disease progression correlates with instability of mutant SOD1 in familial ALS. Neurology 65:1954-1957.

Shibata N, Hirano A, Kobayashi M, Siddique T, Deng HX, Hung WY, Kato T, Asayama K (1996) Intense superoxide dismutase-1 immunoreactivity in intracytoplasmic hyaline inclusions of familial amyotrophic lateral sclerosis with posterior column involvement. J Neuropathol Exp Neurol 55:481-490.

Smith BN, Topp SD, Fallini C, Shibata H, Chen HJ, Troakes C, King A, Ticozzi N, Kenna KP, Soragia-Gkazi A, Miller JW, Sato A, Dias DM, Jeon M, Vance C, Wong CH, de Majo M, Kattuah W, Mitchell JC, Scotter EL, Parkin NW, Sapp PC, Nolan M, Nestor PJ, Simpson M, Weale M, Lek M, Baas F, Vianney de Jong JM, Ten Asbroek A, Redondo AG, Esteban-Perez J, Tiloca C, Verde F, Duga S, Leigh N, Pall H, Morrison KE, Al-Chalabi A, Shaw PJ, Kirby J, Turner MR, Talbot K, Hardiman O, Glass JD, De Belleroche J, Maki M, Moss SE, Miller C, Gellera C, Ratti A, Al-Sarraj S, Brown RH, Jr., Silani V, Landers JE, Shaw CE (2017) Mutations in the vesicular trafficking protein annexin A11 are associated with amyotrophic lateral sclerosis. Sci Transl Med 9:eaad9157.

Smith BN, Ticozzi N, Fallini C, Gkazi AS, Topp S, Kenna KP, Scotter EL, Kost J, Keagle P, Miller JW, Calini D, Vance C, Danielson EW, Troakes C, Tiloca C, Al-Sarraj S, Lewis EA, King A, Colombrita C, Pensato V, Castellotti B, de Belleroche J, Baas F, ten Asbroek AL, Sapp PC, McKenna-Yasek D, McLaughlin RL, Polak M, Asress S, Esteban-Perez J, Munoz-Blanco JL, Simpson M, van Rheenen W, Diekstra FP, Lauria G, Duga S, Corti S, Cereda C, Corrado L, Soraru G, Morrison KE, Williams KL, Nicholson GA, Blair IP, Dion PA, Leblond CS, Rouleau GA, Hardiman O, Veldink JH, van den Berg LH, Al-Chalabi A, Pall H, Shaw PJ, Turner MR, Talbot K, Taroni F, Garcia-Redondo A, Wu Z, Glass JD, Gellera C, Ratti A, Brown RH, Jr., Silani V, Shaw CE, Landers JE (2014) Exome-wide rare variant analysis identifies TUBA4A mutations associated with familial ALS. Neuron 84:324-331.

Steven U Walkley KS, Kunihiko Suzuki (2008) Lysosomal diseases. In: Greenfield's Neuropathology (Seth Love AP, James Ironside, Herbert Budka, ed), pp 515-599. London: Hodder Arnold.

Teyssou E, Chartier L, Amador MD, Lam R, Lautrette G, Nicol M, Machat S, Da Barroca S, Moigneu C, Mairey M, Larmonier T, Saker S, Dussert C, Forlani S, Fontaine B, Seilhean D, Bohl D, Boillee S, Meininger V, Couratier P, Salachas F, Stevanin G, Millecamps S (2017) Novel UBQLN2 mutations linked to amyotrophic lateral sclerosis and atypical hereditary spastic paraplegia phenotype through defective HSP70-mediated proteolysis. Neurobiol Aging 58:239 e11-239 e20.

Tsai PC, Liao YC, Jih KY, Soong BW, Lin KP, Lee YC (2018) Genetic analysis of ANXA11 variants in a Han Chinese cohort with amyotrophic lateral sclerosis in Taiwan. Neurobiol Aging 72:188 e1-188 e2.

van Rheenen W, Shatunov A, Dekker AM, McLaughlin RL, Diekstra FP, Pulit SL, van der Spek RA, Vosa U, de Jong S, Robinson MR, Yang J, Fogh I, van Doormaal PT, Tazelaar GH, Koppers M, Blokhuis AM, Sproviero W, Jones AR, Kenna KP, van Eijk KR, Harschnitz O, Schellevis RD, Brands WJ, Medic J, Menelaou A, Vajda A, Ticozzi N, Lin K, Rogelj B, Vrabec K, Ravnik-Glavac M, Koritnik B, Zidar J, Leonardis L, Groselj LD, Millecamps S, Salachas F, Meininger V, de Carvalho M, Pinto S, Mora JS, Rojas-Garcia R, Polak M, Chandran S, Colville S, Swingler R, Morrison KE, Shaw PJ, Hardy J, Orrell RW, Pittman A, Sidle K, Fratta P, Malaspina A, Topp S, Petri S, Abdulla S, Drepper C, Sendtner M, Meyer T, Ophoff RA, Staats KA, Wiedau-Pazos M, Lomen-Hoerth C, Van Deerlin VM, Trojanowski JQ, Elman L, McCluskey L, Basak AN, Tunca C, Hamzeiy H, Parman Y, Meitinger T, Lichtner P, Radivojkov-Blagojevic M, Andres CR, Maurel C, Bensimon G, Landwehrmeyer B, Brice A, Payan CA, Saker-Delye S, Durr A, Wood NW, Tittmann L, Lieb W, Franke A, Rietschel M, Cichon S, Nothen MM, Amouyel P, Tzourio C, Dartigues JF, Uiterlinden AG, Rivadeneira F, Estrada K, Hofman A, Curtis C, Blauw HM, van

der Kooi AJ, et al. (2016) Genome-wide association analyses identify new risk variants and the genetic architecture of amyotrophic lateral sclerosis. Nat Genet 48:1043-1048.

Wang J, Guo C, Liu S, Qi H, Yin Y, Liang R, Sun MZ, Greenaway FT (2014) Annexin A11 in disease. Clin Chim Acta 431:164-168.

Wang K, Li M, Hakonarson H (2010) ANNOVAR: functional annotation of genetic variants from high-throughput sequencing data. Nucleic Acids Res 38:e164.

Weichert A, Besemer AS, Liebl M, Hellmann N, Koziollek-Drechsler I, Ip P, Decker H, Robertson J, Chakrabartty A, Behl C, Clement AM (2014) Wild-type Cu/Zn superoxide dismutase stabilizes mutant variants by heterodimerization. Neurobiol Dis 62:479-488.

Williams KL, Topp S, Yang S, Smith B, Fifita JA, Warraich ST, Zhang KY, Farrawell N, Vance C, Hu X, Chesi A, Leblond CS, Lee A, Rayner SL, Sundaramoorthy V, Dobson-Stone C, Molloy MP, van Blitterswijk M, Dickson DW, Petersen RC, Graff-Radford NR, Boeve BF, Murray ME, Pottier C, Don E, Winnick C, McCann EP, Hogan A, Daoud H, Levert A, Dion PA, Mitsui J, Ishiura H, Takahashi Y, Goto J, Kost J, Gellera C, Gkazi AS, Miller J, Stockton J, Brooks WS, Boundy K, Polak M, Munoz-Blanco JL, Esteban-Perez J, Rabano A, Hardiman O, Morrison KE, Ticozzi N, Silani V, de Belleroche J, Glass JD, Kwok JB, Guillemin GJ, Chung RS, Tsuji S, Brown RH, Jr., Garcia-Redondo A, Rademakers R, Landers JE, Gitler AD, Rouleau GA, Cole NJ, Yerbury JJ, Atkin JD, Shaw CE, Nicholson GA, Blair IP (2016) CCNF mutations in amyotrophic lateral sclerosis and frontotemporal dementia. Nat Commun 7:11253.

Wu CH, Fallini C, Ticozzi N, Keagle PJ, Sapp PC, Piotrowska K, Lowe P, Koppers M, McKenna-Yasek D, Baron DM, Kost JE, Gonzalez-Perez P, Fox AD, Adams J, Taroni F, Tiloca C, Leclerc AL, Chafe SC, Mangroo D, Moore MJ, Zitzewitz JA, Xu ZS, van den Berg LH, Glass JD, Siciliano G, Cirulli ET, Goldstein DB, Salachas F, Meininger V, Rossoll W, Ratti A, Gellera C, Bosco DA, Bassell GJ, Silani V, Drory VE, Brown RH, Jr., Landers JE (2012) Mutations in the profilin 1 gene cause familial amyotrophic lateral sclerosis. Nature 488:499-503.

Zhang K, Liu Q, Liu K, Shen D, Tai H, Shu S, Ding Q, Fu H, Liu S, Wang Z, Li X, Liu M, Zhang X, Cui L (2018) ANXA11 mutations prevail in Chinese ALS patients with and without cognitive dementia. Neurol Genet 4:e237.

Tables

Mutations	SIFT	Polyphen2 (score)	CADD Phred score	Mutation Taster	Panther	rs number in dbSNP	MAF in gnomAD (%)	MAF in ALSdb (%)	MAF in Project MinE (%)
c.112G>A, p.Gly38Arg	Deleterious	Probably damaging (1.000)	23.6	Disease causing	Probably damaging	rs142083484	All: 0.0042 NFE: 0.0077	0.06	Cases : 0.09 Controls : 0
c.118G>T, p.Asp40Tyr	Deleterious	Probably damaging (0.997)	24.4	Disease causing	Possibly damaging	No	No	No	No
c.629G>A, p.Arg210Gln	Deleterious	Probably damaging (0.996)	31	Disease causing	Probably damaging	rs147610631	All: 0.11 Latino: 0.29 NFE: 0.10	0.06	Cases: 0.034 Controls: 0.027
c.760C>G, p.Leu254Val	Deleterious	Probably damaging (0.991)	25.8	Disease causing	Probably damaging	No	No	No	No

Table 1. Pathogenicity prediction tests for *ANXA11* variants.
Five software packages investigating in silico pathogenicity have been used to classify variants from benign (tolerated) to disease causing (deleterious, probably damaging). A variant with a CADD score >20 indicates that it is among the 1% most deleterious variants in the genome and >30 among the 0.1% (Rentzsch et al., 2019). Minor Allele Frequency (MAF) in gnomAD control populations and dbSNP identification number are indicated. MAF for ALS patients in ALSdb and Project MinE are specified. CADD, Combined Annotation-Dependent Depletion; dbSNP, Single Nucleotide Polymorphism Database; MAF, Minor Allele Frequency; NFE, Non-Finnish European; ALSdb, ALS Data Browser.

Variant	Pedigree	Patients	Age at onset (y)	Site of onset	ALS duration (mo)	pyramidal signs	cognitive signs	Rare variants in other rare ALS genes
p.G38R	FALS1	II1	68	UL	20	++	FTD	No
	FALS1	III1	60	UL+LL	10	+++	Cognitive impairments	NA
	SALS1		61	UL	46	+++	FTD	No
p.D40Y	FALS2	II1	56	LL	67	+++	FTD	No
	FALS2	II2	69	Bulbar	49	++	FTD	No
p.R210Q	FALS3	II1	70	Bulbar	9			*TBK1*, c.427C>T, p.Arg143Cys
	FALS4	II1	69	Bulbar	34			*GLE1*, c.1858A>G, p.Thr620Ala
p.L254V	SALS2		33	UL	34			No

Table 2. Clinical features of patients harboring *ANXA11* mutations.
ALS, amyotrophic lateral sclerosis; FTD, Frontotemporal Dementia; UL, upper limb; LL, lower limb; NA, not applicable (DNA was not available).
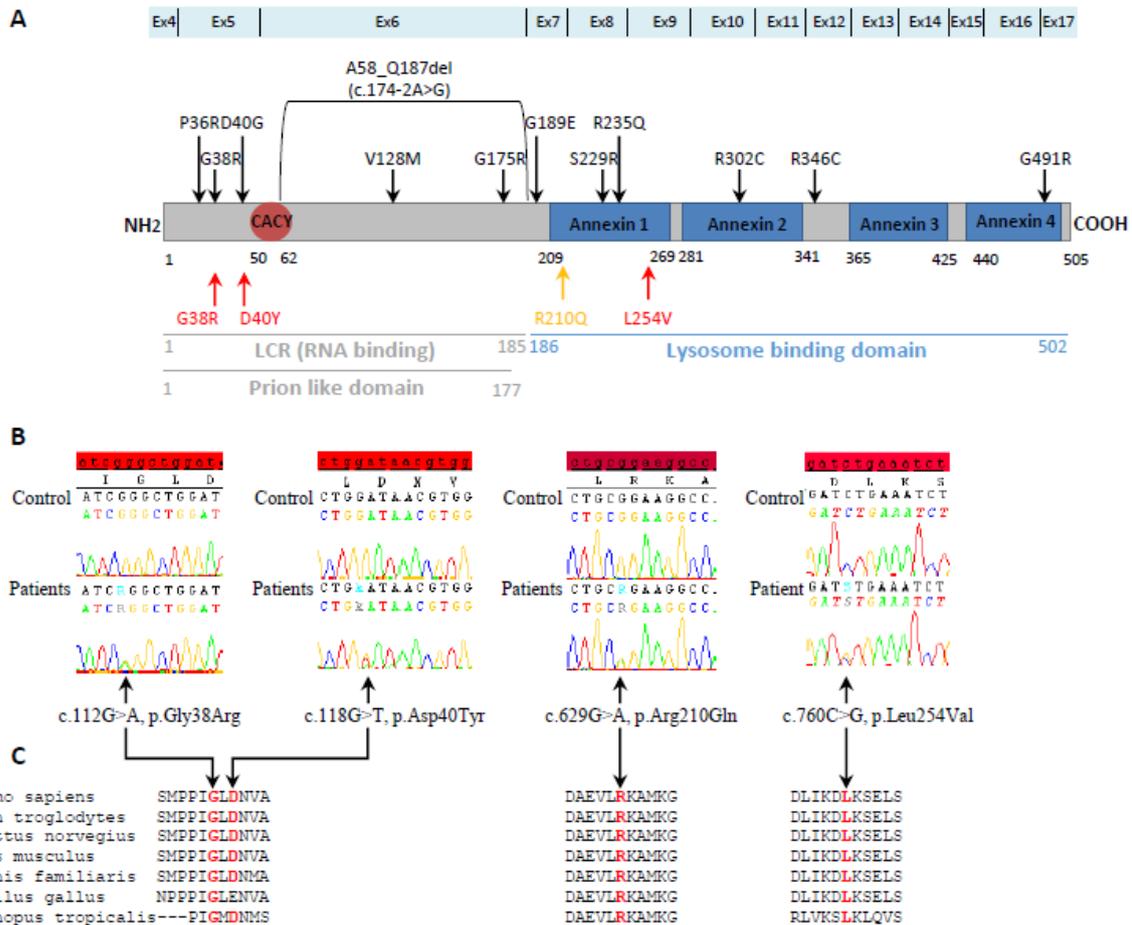
Figures

Fig. 1. Identification of *ANXA11* mutations in patients with ALS.
Representation of the 14 exons of *ANXA11* and of Annexin A11 protein domains with the position of mutations previously reported in ALS patients in black (A). Data are compiled from Smith *et al.*, 2017; Tsai *et al.*, 2018 ; Zhang *et al.*, 2018 ; Liu *et al.*, 2019. The 3 pathogenic mutations identified by exome analysis in our study are in red and the R210Q variant of unknown significance is in orange**.** The p.G38R mutation was already described. A Prion-like domain (gray) was determined by the software PLAAC (Prion Like Amino Acid Composition). RNA (gray) and lysosome (blue) binding domains are represented. The binding site with calcyclin/S100A6 (CACY) is located at N terminal. The four highly conserved annexin domains are represented by blue square. Part of chromatograms showing the p.G38R (exon 5) and p.D40Y (exon 5), the p.R210Q (exon 7) and the p.L254V (exon 9) variants pointed by an arrow (in patients) and the corresponding normal sequences (in control) (B). Sequence alignment of part of the Annexin A11 amino acids from diverse species. The positions of Gly38, Asp40, Arg210 and Leu254 (pointed by an arrow) are in red. Sequences used include *Homo sapiens* (NP_001265338.1), *Pan troglodytes* (XP_507872.4), *Rattus norvegius* (NP_001011918.1), *Mus musculus* (NP_038497.2), *Canis familiaris* (XP_536312,2), *Gallus gallus* (NP_001012921.2), *Xenopus tropicalis* (NP_001006124.1) (C).
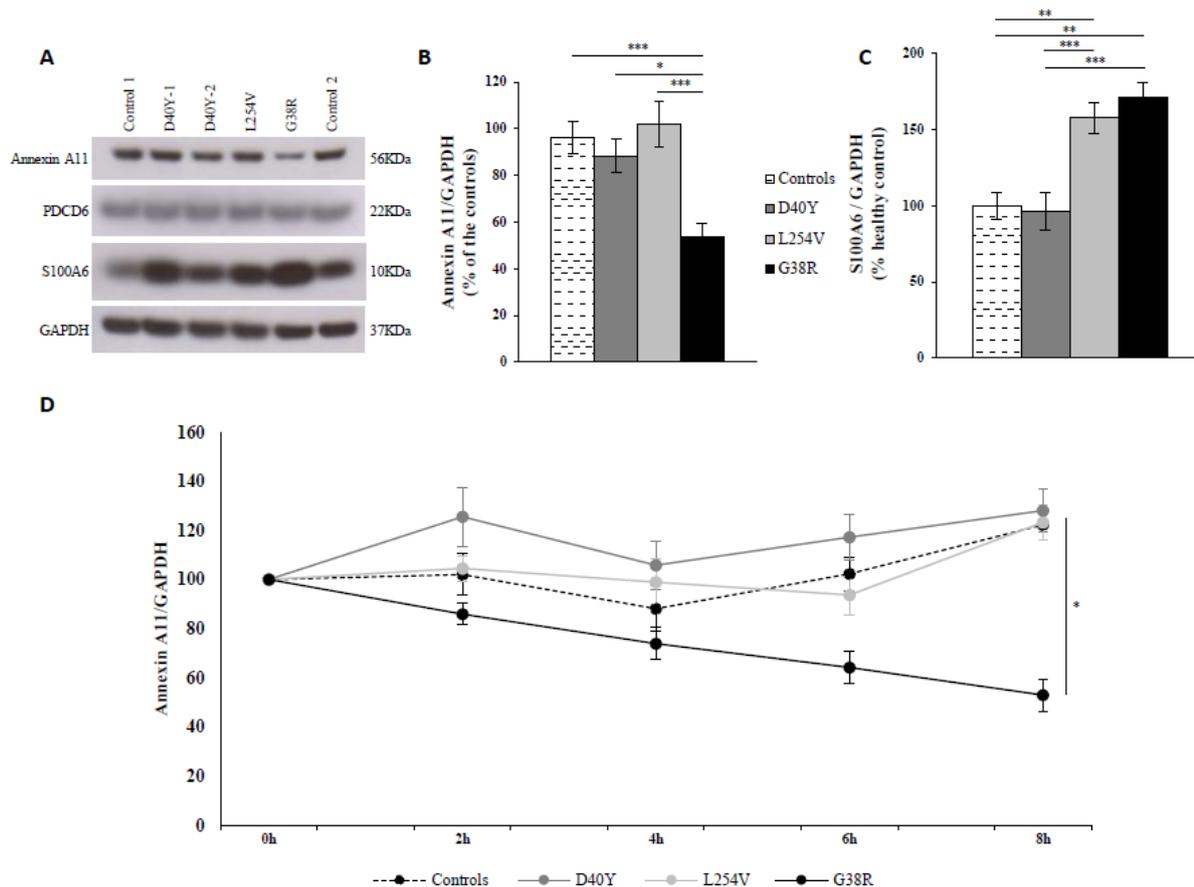
Fig. 2. p.G38R mutation impairs Annexin A11 stability and protein levels.
Immunoblots analyses of lymphoblasts extracts from control and ALS patients carrying the p.G38R, p.D40Y or p.L254V *ANXA11* mutations using anti-Annexin A11, anti-PDCD6, anti-S100A6 and anti-GAPDH antibodies (A). Densitometry analyses of Annexin A11 (B) and S100A6 (C) for control (hatched) and patients with p.D40Y (dark grey), p.L254V (light grey) or p.G38R (black) mutation. Data (represented as percentage of the control) are means ± standard errors of the mean (SEM) of 6 to 24 values from 6 to 12 independent experiments. Kinetic curves showing the rate of degradation of Annexin A11 in lymphoblasts of healthy controls (hatched), p.D40Y patients (dark grey), p.L254V patient (light grey) and p.G38R patient (black) in the presence of cycloheximide. Results are means +/- SEM of 11 experiments and are presented as percentage of initial protein (D). *p < 0.05, **p <0.01, ***p <0.005.
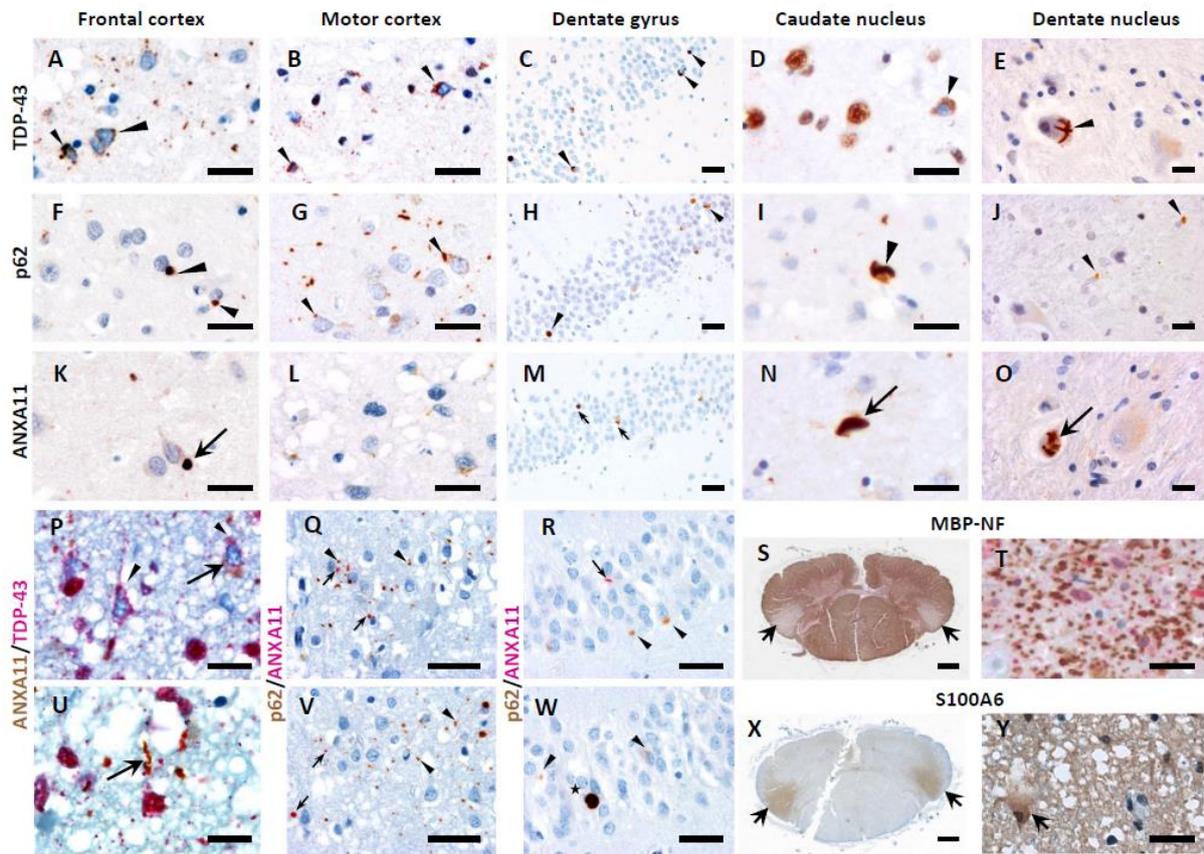
Fig. 3. Neuropathological analysis of ALS patient tissue with the p.G38R *ANXA11* mutation.

Post-mortem tissue sections (midfrontal cortex, motor cortex, dentate gyrus of the hippocampus, head of the caudate nucleus and dentate nucleus of the cerebellum) were stained with anti-phosphorylated TDP-43 (A-C), anti-TDP-43 (D-E), anti-p62 (F-J) and anti-Annexin A11 (K-O). Numerous deposits of phosphorylated TDP-43 were detected in neurons and glial cells of the frontal (A) and the motor (B) cortex and were less numerous in the dentate gyrus of the hippocampus (C). Cytoplasmic TDP-43 was observed in some neurons of the caudate nucleus (D, arrowhead). Some p62 positivities were also detected in the same regions (F-I). Annexin A11 accumulations were detected in all these brain regions (K-N). In the dentate nucleus of the cerebellum, neuronal cytoplasmic inclusions of TDP-43 (E) and Annexin A11 (O) and glial dot-like p62 positivities (J) were also detected. Macroscopic analysis showed severe lateral tractus degeneration using MBP-NF staining (arrows in S, T) associated with S100A6 diffuse staining (arrows in X, Y). Double staining for Annexin A11 (brown, arrows) and TDP-43 (red, arrowheads) in the frontal cortex showed separate localization of both markers in the same cells with no superposition (P, U). Note the neuritic accumulation of Annexin A11 in U. Double staining for Annexin A11 (red, arrows) and p62 (brown, arrowheads) in the motor cortex (Q, V) and the dentate gyrus of the hippocampus (R, W) also showed separate localizations. Rare inclusions presented superposition (star in W). Scale bars: 10 µm (A-O, P-R, U-W) and 1 mm (S, X).
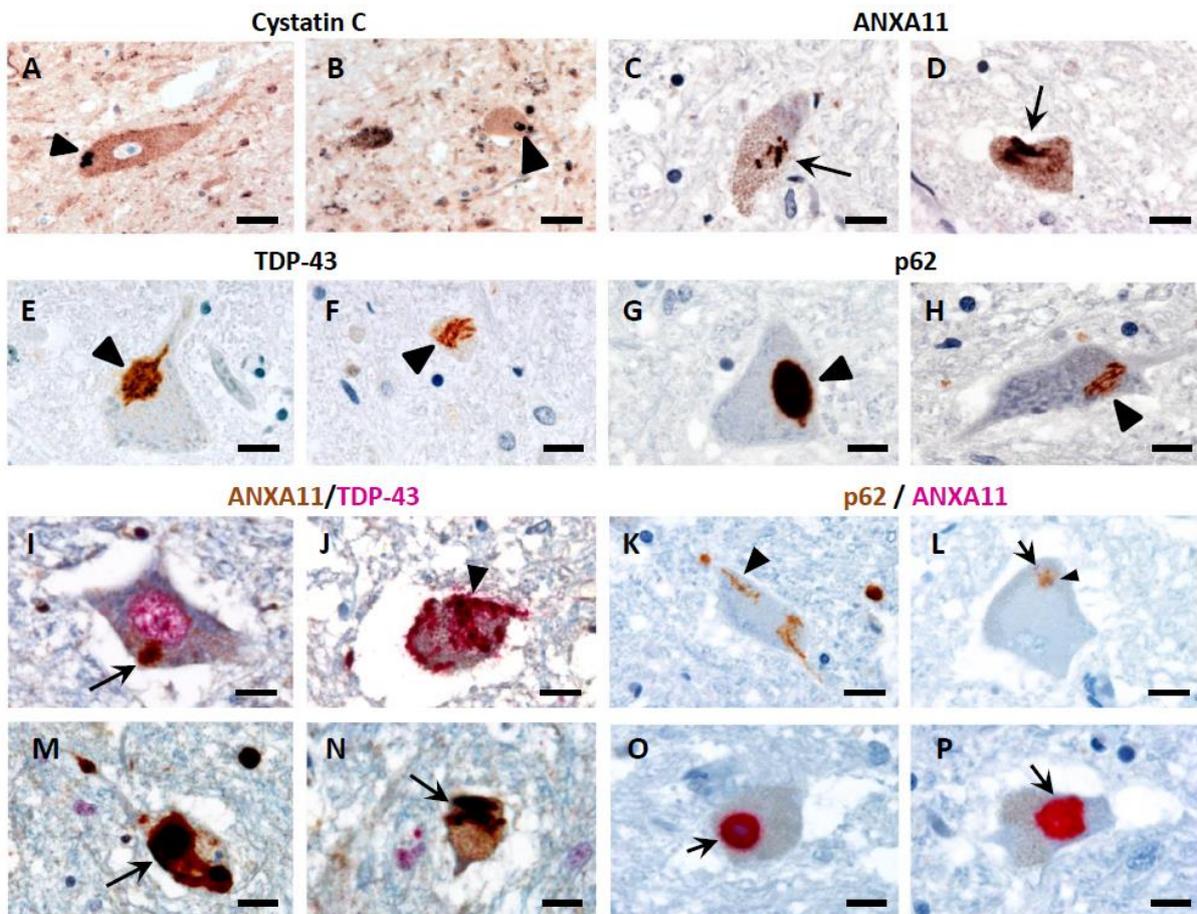
Fig. 4. Protein inclusions detected in ALS spinal cord with the p.G38R *ANXA11* mutation.
Post-mortem spinal cord sections were stained with anti-Cystatin C (A, B), anti-Annexin A11 (C, D), anti-phosphorylated TDP-43 (E, F) and anti-p62 (G, H). Classical ALS hallmarks (arrowheads) were observed in the spinal motor neurons including Bunina bodies (A, B) and large skein-like aggregates, positive for phosphorylated TDP-43 (E, F) and p62 (G, H). ANXA11 inclusions (arrows) were detected in motor neurons (C, D). Double staining for Annexin A11 (brown, arrows) and TDP-43 (red) showed the presence of Annexin A11 deposits in motor neurons having retained their nuclear TDP-43 (I), large conglomerates of TDP-43 (J, arrowhead) and large conglomerates of Annexin A11 with superposition (M, N). Double staining for Annexin A11 (red, arrows) and p62 (brown, arrowheads) showed p62 inclusions in absence of Annexin A11 deposits (K), coexistence of thin Annexin A11 deposits and p62 in the same motor neuron without evidence of superposition (L) or large round inclusions of Annexin A11 (O, P). Scale bars: 10 µm.
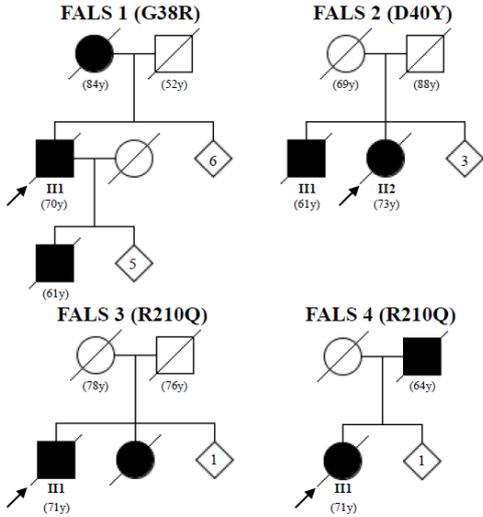
Supplemental Files

Fig. S1. Pedigrees of the families with *ANXA11* mutations.
Arrows indicate index patients. When available, the age at death (in brackets) is indicated under the symbol representing the patients. Black fill: Amyotrophic Lateral Sclerosis (ALS) case.
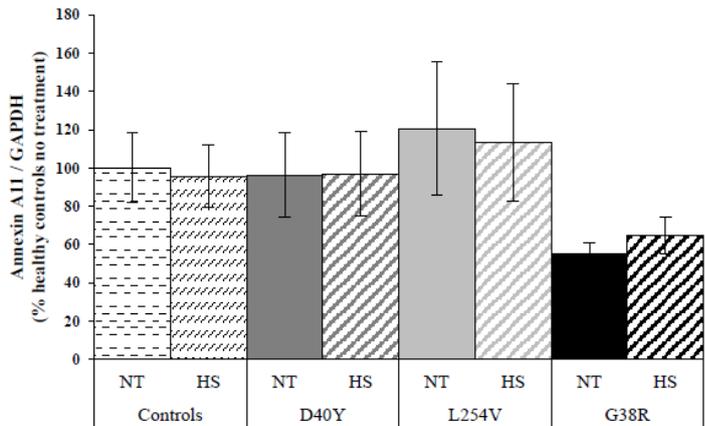

Fig. S2. Annexin A11 levels are not modified after heat shock stress.
Densitometry analyses of Annexin A11 levels after heat shock for controls (hatched) and ALS patients carrying the p.D40Y (dark gray), p.L254V (light gray) or G38R (black) *ANXA11* mutations. Data are means ± SEM of 2-4 values from 2 independent experiments. Annexin A11 levels were standardized to GAPDH levels. NT: no treatment; HS: heat shock.
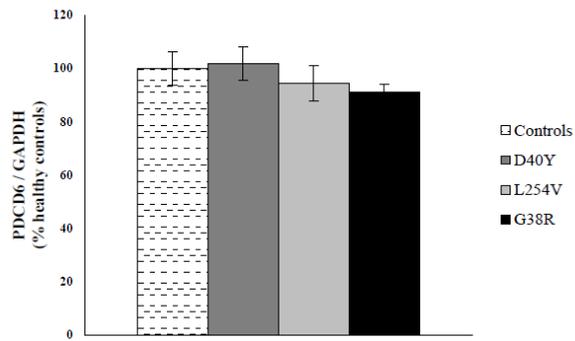
Fig. S3. PDCD6 levels are not modified in lymphoblasts with ANXA11 mutations compared to controls.
Densitometry analyses of PDCD6 for controls (hatched) and ALS patients carrying the p.D40Y (dark gray), p.L254V (light gray) or G38R (black) ANXA11 mutations. Data are means ± SEM of 4-8 values from 4 independent experiments. PDCD6 levels were standardized to GAPDH levels.